POROSITY MAPPING FROM INVERSION OF POST-STACK SEISMIC DATA

B. Das, R. Chatterjee
Indian Institute of Technology (Indian School of Mines), Dhanbad, India

Abstract. A seismic section oriented N-S passing through well "W" is considered for porosity prediction in offshore of Krishna-Godavari (K-G) basin. The gamma ray log trend indicates deposition of cleaning upward sediment. Coarsening upward, clayey-silty-sandy bodies, making a series of about 50-60 m thickness, have been evidenced from the gamma ray log. Porosity is mapped from transformation of acoustic impedance (AI). Post-stack inversion of seismic data is routinely carried out to derive AI and hence petrophysical properties in an area. We have been introducing here an uncommon approach of inverting post-stack seismic data into porosity from porosity log. The post-stack inversion for estimation of direct porosity is performed by utilizing an estimated porosity wavelet, low frequency model and model based inversion. This approach is implemented on clay rich, shaly sediments in shallow offshore. The total porosity for the depth interval of 1200-1600 m ranging from 1 to 40 % has been used as input for porosity inversion from the 2D post-stack seismic data of shallow offshore sediments at 31m bathymetry in K-G basin. This prediction is applied to dataset having good correlation between AI and porosity. In K-G basin, the porosity in Raghavapuram Shale varies from 13 to 30 % with maximum value of 40 % is observed in Paleocene sediments. The shales/unconsolidated sediments measure a high porosity with low impedance and the more porous sands are in an intermediate range. The predicted impedance and porosity values may be erroneous beyond the drilled depth because of non availability of well log data for calibration.

Keywords: Krishna-Godavari basin, Porosity, Seismic Inversion, Raghavapuram Shale
DOI: 10.18599/grs.18.4.8

For citation: Baisakhi Das, Rima Chatterjee Porosity Mapping from Inversion of Post-Stack Seismic Data. *Georesursy = Georesources*. 2016. V. 18. No. 4. Part 2. Pp. 306-313. DOI: 10.18599/grs.18.4.8

1. Introduction

In general conventional seismic interpretation entails picking and tracking laterally consistent seismic reflectors for the purpose of mapping horizon of interest, geological structures, stratigraphy and reservoir architecture. The aim of interpretation is usually to detect hydrocarbon bearing geological bodies, to delineate their extent, and calculate their volumes. Acoustic impedance (AI) mapping is a common approach for inversion of post-stack seismic data to delineate reservoir properties. Nowadays, pre-stack seismic inversion techniques are used for computation of impedances: P-impedance, S-impedance and density. These are further used for estimation of porosity, shale volume, lithofacies and water saturation from seismic data. Well information are available at hundreds of meters apart, therefore the objective of seismic inversion method for reservoir characterization is to delineate petrophysical properties for the interwell region or adjacent to the wells.

Observations on sonic log data provide good vertical resolution of geological strata, but are at sparse locations. In contrast, seismic method provides usual areal sampling but with noticeably lower vertical resolution. The integration of 2D seismic data of any area with porosity measurement at wells can significantly improve the porosity distribution in space. The petrophysical parameters are generally predicted from seismic inversion properties such as AI using multivariate statistics modelling, non-linear methods including neural network (e.g. Hampson et al., 2001; Leiphart, Hart, 2001;Walls et al., 2002; Pramanik et al., 2004; Calderon, 2007; Singha, Chatterjeee 2014; Singha et al., 2014). Objectives of this paper are to (a) transformation of AI to porosity mapping, (b) development of relation between porosity and acoustic reflectivity from post stack seismic data, as well as(c) direct inversion of post-stack seismic data to predict porosity from well log. The methodology is applied to 2D post-stack data of shallow offshore of Krishna-Godavari (K-G) basin.

2. Study area

The pericratonic rifted basin is holding multiple petroleum system aging Mio-Pliocene to Cretaceous age. The shallow offshore area (Figure 1) located at the north-eastern part of K-G basin is considered for porosity prediction from 2D post-stack seismic data.The study area contains sediments of Gollapalli Sandstone, Tirupati Sandstone and Raghavapuram Shale formations of Cretaceous age. The sands are deposited during the Upper Cretaceous by a prograding deltaic system that spread out into shelf and slope environments. The shallow marine environment with very slow rate of sedimentation, shallow bathymetry and the

nearness to the provenance result the deposition of high gamma-high resistivity shale (HG-HR) sequence known as Raghavapuram Shale (Manmohan et al., 2003). The sequence is carbonaceous, organic rich, silty and with high radioactive: thorium and potassium content. The porosity estimation of Raghavapuram Shale in shallow water is very critical in reducing the drilling risk in this trend. Because the sandstones present in this formation tend to be thin and inter-bedded with shale, the high reflectivity has a dimming effect on the reflection images of sand-shale boundaries in this zone.

The seismic section belonging to shallow offshore of K-G basin show the geological horizon with its age (Figure 2). The faults are identified in the seismic section. The Paleocene top is observed at 420 ms. Seismic reflections are mainly attributed to unconsolidated silty sand/shale/mudstone occurring 400-580 ms of Paleocene age. Top of Raghavapuram Shale is observed at 850ms from seismic section of K-G basin. Top of Cretaceous and basement of Permian age are observed around 580 ms and 1200 ms respectively. The penetration of seismic energy into the underlying basement is significantly reduced. The basement top stands out as a prominent reflector between the overlying bedded sediments and underlying noisy section of the basement.

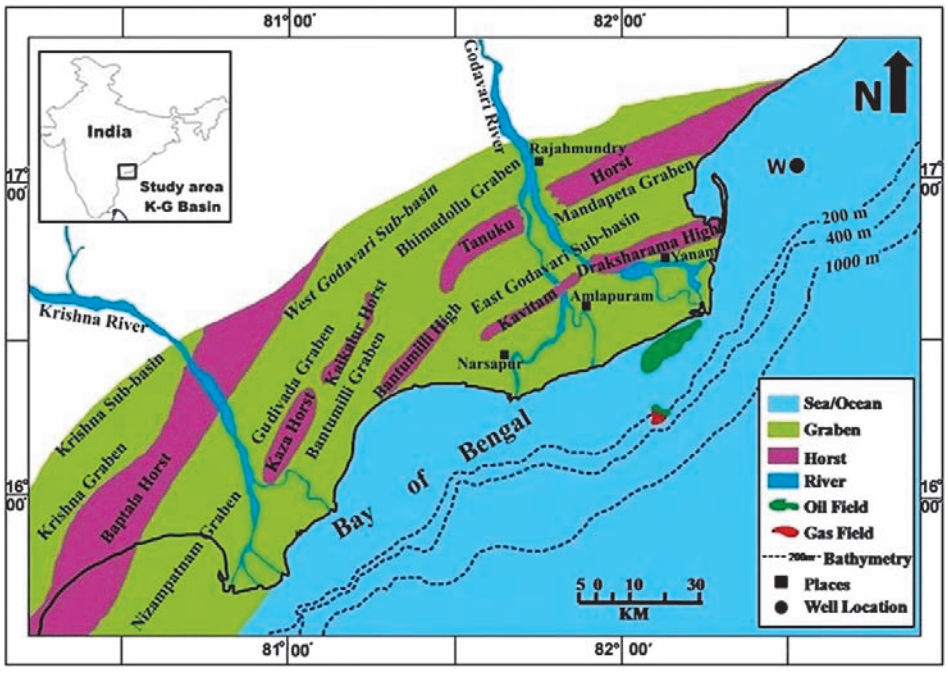

Figure 1. Location map of Krishna-Godavari (K-G) basin along eastern continental margin of India.

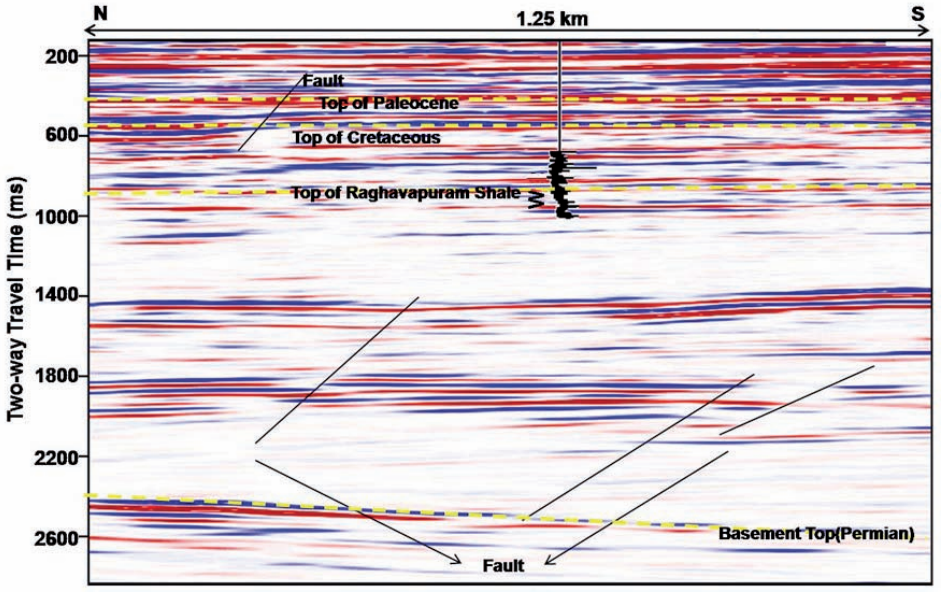

Figure 2. Interpreted seismic section containing a well "W" of K-G basin.

Depositional environment from Well log

The depositional environment of Early Cretaceous formation is of fluvio-deltaic setting with good sands development in channels and delta distributaries. The Late Cretaceous formations areof shallow marine setting with sand developments mostly in tidal channels, bars and sandy flats (Rao, 2001 and Shrivastva et al., 2008).The gamma ray and resistivity logs are called typicallithologyindicative logs for siliciclastic environments (Eichkitz et al., 2009). The log shapes in gamma ray with resistivity are related to sediment character and depositional environment (Rider, 2002). Shapes on the gamma ray log can be interpreted as grain size trends and by sedimentological association as cycles. Information about the sediments and sedimentary processes from the above logs may not be sufficient alone, due to some lithologies having similar natural radioactivity and electrical properties. Information from cuttings and cores is therefore often an essential component of depositional environmental analysis (Jipa, 2012). Figure 3 displays variable sandstone/silty sand body thickness patterns; including thick to thin, blocky to upward-fining log characters at greater depths (Figure 3). The gamma ray log shape in this well "W" and associated seismic signatures display the characteristics of singular or stacked package of sandstone/silty sand bodies of fining upward sequence.

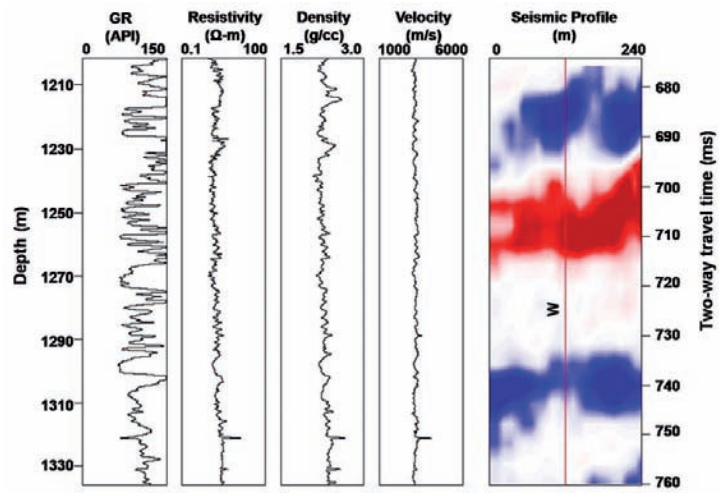

Figure 3. Well logs and corresponding seismic data from well "W" showing different depositional environment in the depth interval of 1200-1335 m. Red, peak of seismic trace and blue, trough of trace.

The shallow marine environment, shallow bathymetry, very slow rate of sedimentation and the nearness to the provenance resulted in the deposition of high gamma-high resistivity shale (HG-HR) sequence (Manmohan et al., 2003). The sequence is carbonaceous, organic rich, silty and with high thorium and potassium content.

3. Post-stack Seismic Inversion:

3.1 Transformation of AI to Porosity mapping

Post-stack seismic inversion has been widely used in the petroleum industry for subsurface geological inferences (e.g., lithology, porosity) based on seismic analysis tied to well logs (i.e., resistivity, sonic and density). The method increasingly confirms the usefulness of inverted seismic data and is informative for seismic interpretation (Buiting, Bacon 1999).

Post-stack inversion is used to transform seismic reflection data into acoustic impedance as it uses normal incidence reflections and requires only near-offset stack data (rather than full aperture stacked data) to obtain physically and geologically reliable results. Analysis of post stack seismic data has been used as an effective tool for hydrocarbon exploration in many areas around the world. The goal of seismic inversion procedure in the case of reservoir characterization is to map the physical properties such as porosity, water saturation and lithology for the inter-well regions.

For all seismic inversion methods, the earth can be represented by a stack of plane and parallel layers with constant physical properties (Leite et.al, 2010). The seismic trace s(t) can be represented by the convolution of the reflectivity series r(t) and band-limited wavelet w(t) and addition of random noise n(t). Mathematically seismic trace s(t) can be written as,

$$s(t) = r(t)*w(t)+n(t), \quad (1)$$

The acoustic impedance at ith layer is calculated as,

$$AI_i = \frac{R_{i+1} + R_i}{R_{I+1} + R_i}, \quad (2)$$

where R_i and R_{i+1} is the reflection co-efficient of *i*th and *i+1*th layer respectively.

Russel (1991) defines the model based inversion as an iterative modeling scheme in which the geological model is built and compared to the seismic data and the comparison is used to iterate to get the better model. The inversion requires the initial value of impedance. An initial model for the model based inversion is generated using the acoustic impedance logs calculated at the well location. The inversion algorithm modifies the impedance log to minimize the misfit between the measured and synthetic seismic data. As it is to be expected with impedance inversion, a good match between seismic and synthetic data can be achieved. Figure 4 is showing the match between the inverted impedance and well log data for two sections under the study area. The inverted acoustic impedance for the section is illustrated in Figure 5. The inverted impedance section around the well "W" is showing the low impedance at 800-900 ms.

The inversion methods require seismic data, low frequency model and a wavelet estimated from the data.

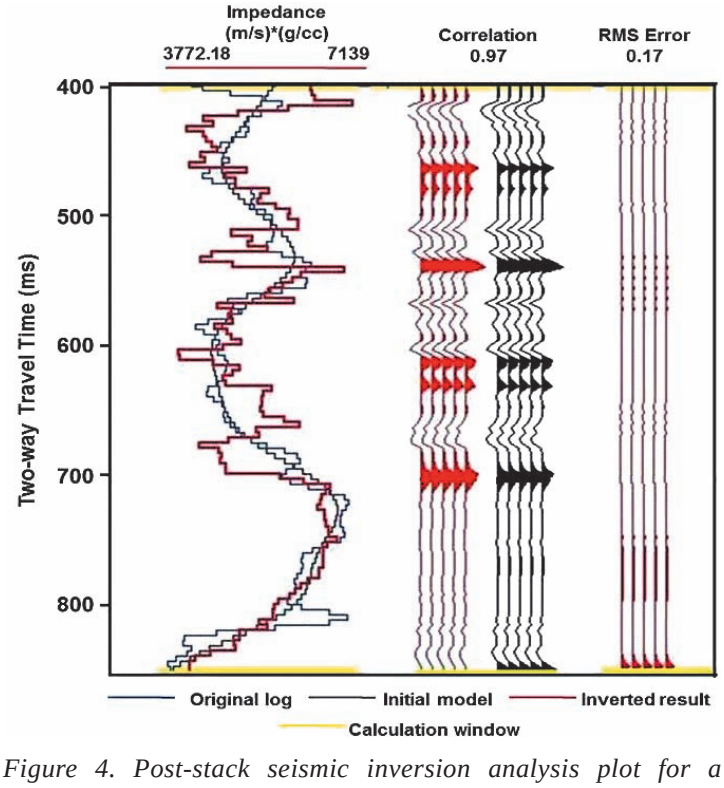

Figure 4. Post-stack seismic inversion analysis plot for a seismic line showing matching between the inverted (red line) and computed acoustic (blue line) impedance within calculation window (yellow line). The black curve indicates the low frequency impedance extracted from the observed impedance logs. The red and black seismic traces are the synthetic and real seismic data respectively.

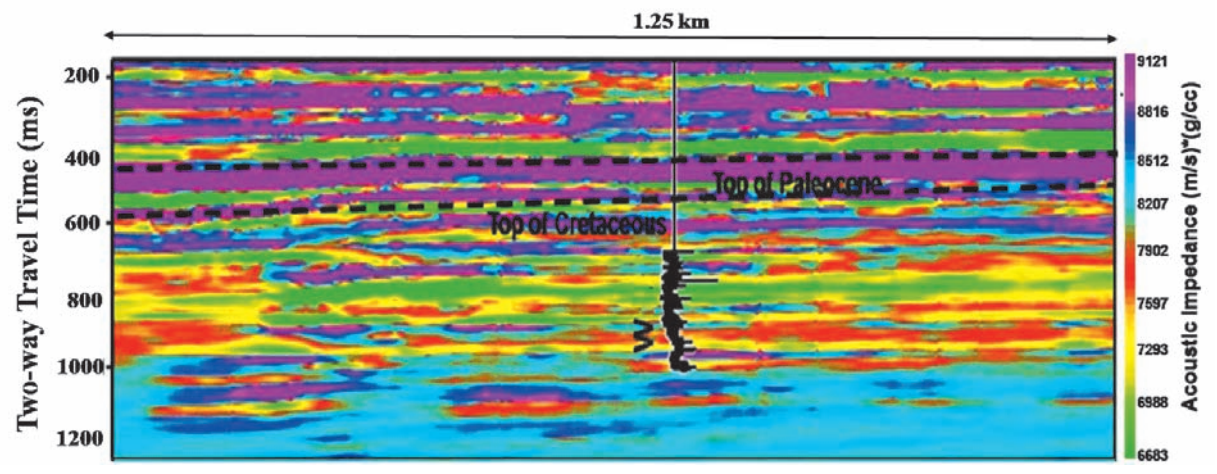

Figure 5. Inverted seismic section with lateral variation in acoustic impedance for the seismic section.

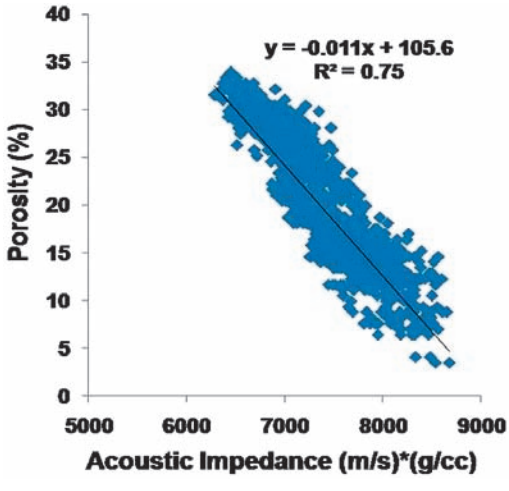

Figure 6. Crossplot between Acoustic impedance and density derived porosity for K-G basin showing good fit (R^2=0.75) to linear trend of lithology.

For accurate wavelet estimation P wave log is used for calibration of seismic data (Singha et al., 2014). A common way to extract porosity from seismic data is to employ acoustic impedance inversion. One can estimate porosity from the inverted AI using mathematical relation between AI and porosity derived from well log. Figure 6 is showing the best linear fit with goodness of fit (R^2=0.75) between AI and density derived porosity for the well "W". Density porosity is derived from the following equation (after Bateman, 1985):

$$\varphi_d = \frac{\rho_m - \rho_{\log}}{\rho_m - \rho_f}, \quad (3)$$

where ρ_m, ρ_f and $\rho_{\log}$ are the matrix density, fluid density and the bulk density of formation respectively. Here matrix density and fluid density are considered as 2.65g/cc and 1.1g/cc respectively.

The inverted acoustic impedance is transformed into porosity from the relations obtained from cross plot (Figure 6) using following equations (4) for seismic section.

Porosity = -0.011(AI) +105.6 (4)

Figure 7 is showing the porosity image of the seismic section.

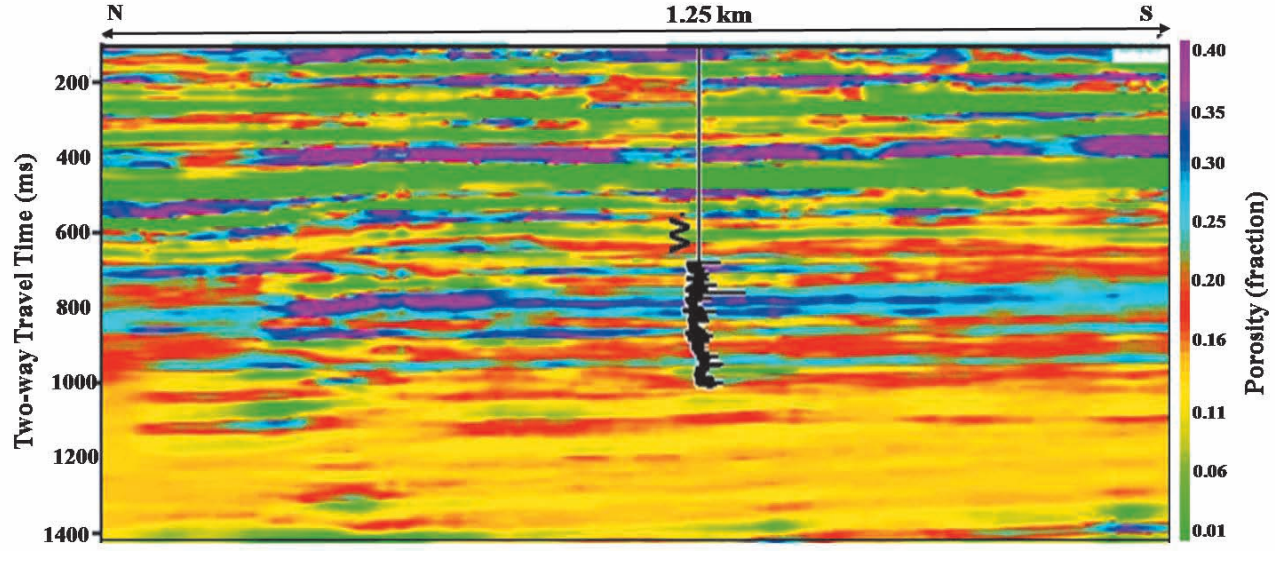

Figure 7. Inverted porosity section for the seismic section using transformation of AI to Porosity.

3.2 Direct Inversion of Post-stack Seismic Data to Predict Porosity

A modified approach using idea of AI reflectivity has been used to predict porosity from post-stack seismic inversion. The inversion procedure involves well to seismic calibration, wavelet extraction, estimation of low frequency model and model based inversion for seismic dataset of K-G basin (Maver, Rasmussen, 1995; Husse, Feary, 2005; Kumar et al., 2016). Porosity is computed from density logs available from a offshore well located at K-G basin.

Wyllie et al. (1956) has proposed formula for velocity (v) for porous rock as

$$\frac{1}{\upsilon} = \frac{\varphi}{\upsilon_f} + \frac{1-\varphi}{\upsilon_m} \quad (5)$$

where v_f and v_m denotes fluid and matrix velocity respectively. Assuming density and velocity of the matrix being much larger than respective values of the fluid, the AI (denoted by z) of the porous rock is given by (Rasmussen, Maver, 1996)

$$\log(z) = \log(\rho_m \cdot \upsilon_f) - \log\left(\frac{\varphi}{1-\varphi}\right) \quad (6)$$

Conversely, if the density and velocity of the matrix are not considered being much larger than respective value of fluids, we can expect less sensitivity of AI with respect to the porosity. Rasmussen and Maver (1996) provide a model between AI and porosity as given below:

$$\log(z) = \log(z_0) + n\log\left(\frac{\varphi}{1-\varphi}\right) \quad (7)$$

where z_0 and n denotes intercept and slope respectively.

The reflection coefficient is called AI reflectivity between layer *i* and *i+1* as given by Rasmussen and Maver (1996)

$$r_z = \frac{1}{2}\left(\log(z_{i+1}) - \log(z_i)\right) \quad (8)$$

And porosity reflectivity is defined as

$$r_\varphi = \frac{1}{2}\left(\log\left(\frac{\varphi_{i+1}}{1-\varphi_{i+1}}\right) - \log\left(\frac{\varphi_i}{1-\varphi_i}\right)\right) \quad (9)$$

$\log(z_0)$ of equation (7) contributes negligibly compared to $n\log(\varphi/(1-\varphi))$. Hence, the relation between porosity and AI reflectivity can be expressed by (Rasmussen, Maver, 1996, Kumar et al., 2016)

$$r_z = n r_\varphi \quad (10)$$

Equation (10) is used statistically for determining the slope, "n", referred to as correlation factor among AI and porosity reflectivity using log values. The case study from K-G basin will show the relation between porosity and AI reflectivity.

The AI and porosity logs are used for estimation of wavelet and low frequency models. Therefore, porosity wavelet is generated by multiplying the AI wavelet (computed from density and velocity logs) with the correlation factor. The estimated wavelet and a low frequency model enable the execution of seismic inversion. The accuracy of model based seismic inversion (Russell, Hampson, 1991) relies on the low frequency model which is determined by the root mean square (RMS) error between the well logs and the inverted AI or porosity.

3.3 Porosity Prediction in K-G basin

Shrivastava et al. (2008) have explained the geological structures with the identified hydrocarbon prospects on N-S seismic section passing through our study area. Figure 6 is showing the linear trend of the lithology between AI and density derived porosity with good fit of R^2 =0.75 for shallow offshore well in K-G basin. The porosity inversion using porosity reflectivity may be a good option for this type of dataset.

P-wave velocity and porosity varies from 2814 to 4090 m/s and 1 to 40 % respectively. The AI reflectivity from impedance log and porosity reflectivity from

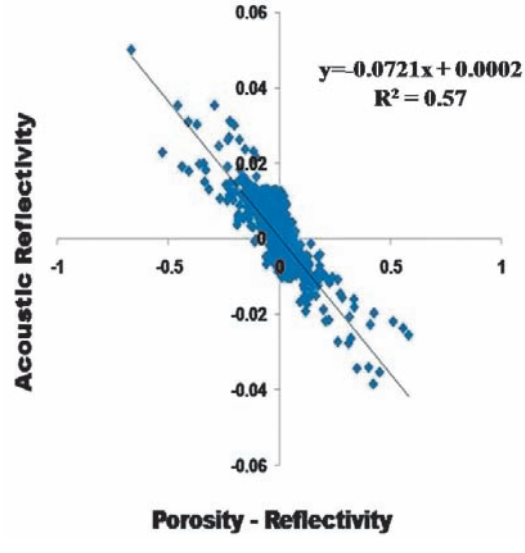

Figure 8. Crossplot between Acoustic reflectivity and Porosity reflectivity for K-G basin showing good fit which decides the correlation factor (n = -0.0721).

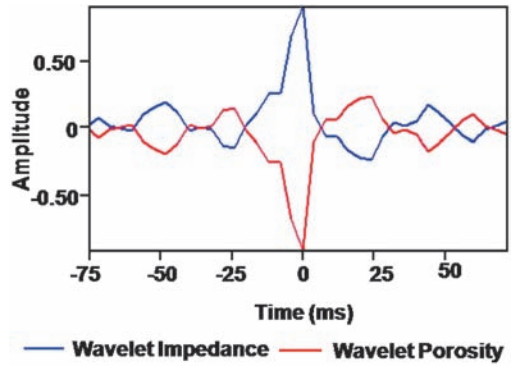

Figure 9. Extracted acoustic impedance wavelet (blue) and porosity wavelet (red) showing opposite polarity to each other for K-G basin.

porosity log using equations (8) and (9) are again computed respectively for this basin. The plot between AI and porosity reflectivity for this well at K-G basin is displayed in Figure 8.

The estimated AI and porosity reflectivity is showing a linear relationship,

$$r_z = -0.0721 r_\varphi \quad (11)$$

From above relation value of correlation "n" is found to be -0.0721. The porosity wavelet is derived from multiplication of AI wavelet with this factor.

We have derived a wavelet from seismic section of 1.25 km within the time interval 800-1000 ms (Figure 9). Porosity wavelet is generated using equation (11) from AI wavelet as shown in Figure 9.

The model based inversion is carried out to predict porosity using porosity inversion. The error analysis for inverted output and original logs are shown in Figure 10 a, b. The inverted porosity for this seismic section of K-G basin are shown in Figures 11.

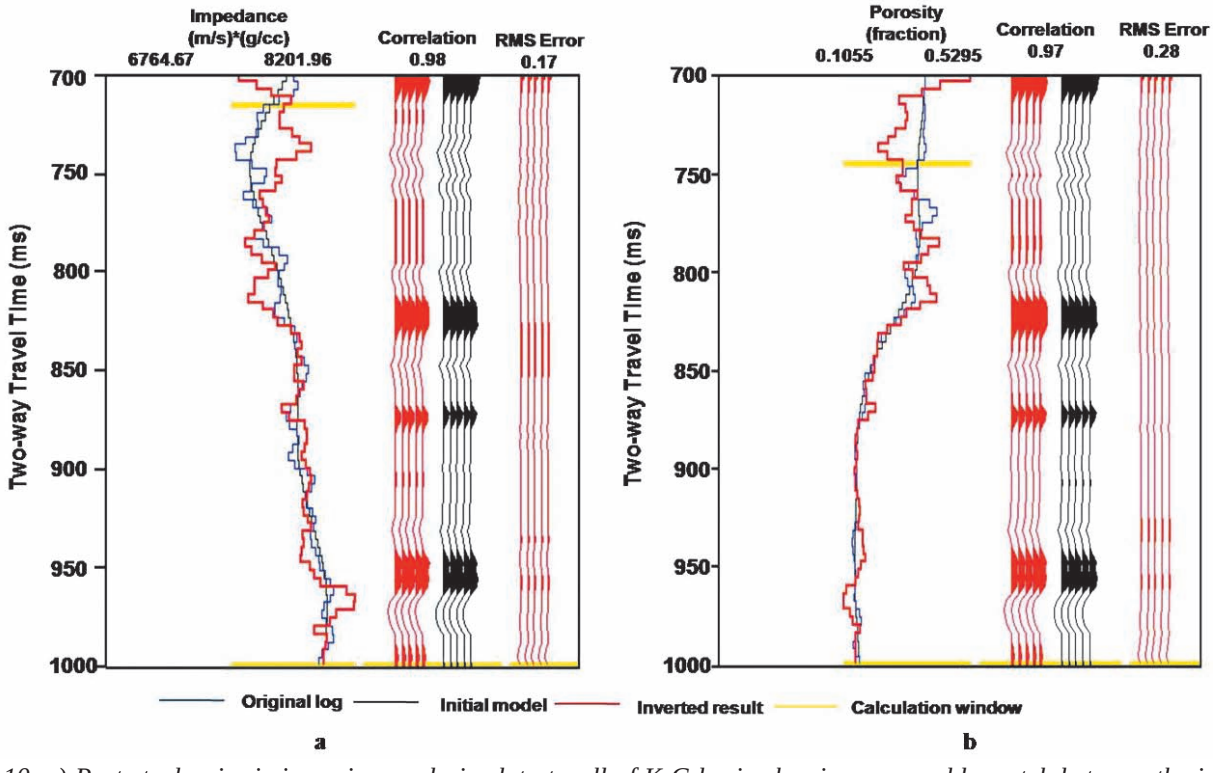

Figure 10. a) Post-stack seismic inversion analysis plot at well of K-G basin showing reasonable match between the inverted (red line) and computed acoustic impedance (blue line) within a calculation window (yellow line). The black curve indicates the low frequency impedance extracted from the acoustic impedance log. The red and black seismic traces are the synthetic and real seismic data respectively. b) Post-stack seismic inversion analysis plot at well of K-G basin showing reasonable match between the inverted (red line) and computed porosity log (blue line) within a calculation window (yellow line). The black curve indicates the low frequency impedance extracted from the observed porosity log. The red and black seismic traces are the synthetic and real seismic data respectively.

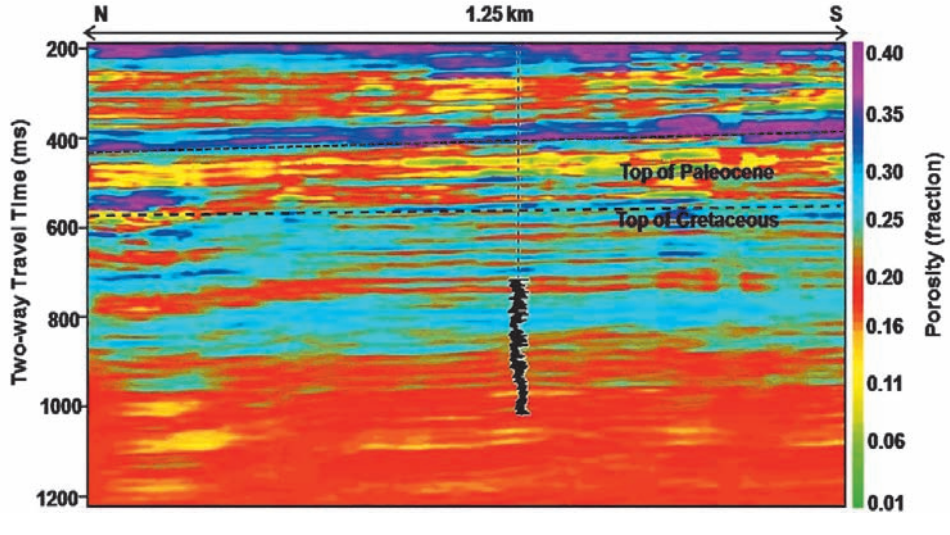

Figure 11. Inverted porosity section using direct inversion of the post-stack seismic section of K-G basin.

4. Results and Discussion

Acoustic impedance in the inverted seismic section varies from 6683 to 9121m/s*gm/c.c. This variation is due to sand, clay, siltstone and shale. Top of Cretaceous is observed in the well "W" at 1150 m and in seismic section around 580ms. Inverted porosity of the seismic sections vary from 1 to 40 % respectively. Porosity section follows the trend of seismic signature and structures of the study area. The high impedance zones observed in the both section having source rock potential show relatively less porosity compared to the porosity of low impedance zones. Lithologies of source rock generally vary across a continuum from wholly organic sediments (such as: coal), through siliciclastic shales and marls, to carbonates (Lφseth et al., 2011). High silica and carbonate content results in high impedance shales (Prasad et al., 2002). High gamma and high resistivity (5-10 ohm-m) Raghavapuram Shale is showing 16 to 35 % from 780 to 1200ms. This observation matches with the log signatures as noted by previous authors (e.g. Padhy et al., 2013). The porosity image of the seismic section in 950-1200 ms is ranging from 15 to 30 % in the Raghavapuram Shale.

This uncommon method of prediction of porosity is implemented to shallow offshore seismic data of K-G. Good fit of R^2=0.75 is observed between AI and porosity in K-G basin. Wavelet of 200 ms long from K-G basin is extracted for seismic calibration to achieve good inversion results. Model based inversion is carried out up to well drilled depth for both methods. RMS error for porosity prediction is found to be 0.28 for K-G basin. Porosity section follows the trends of seismic signature and structures K-G basin. AI varies from 6683 to 8512 m/s*g/cc and porosity ranges from 16 to 25 % characterizing Raghavapuram Shale in K-G basin. The interbedded high amplitude laterally continuous event (within 780 to 1200 ms) may be considered as potential of source rock in Raghavapuram Shale (Figure 11). Raghavapuram Shale is marked very clearly through direct inversion of AI for porosity mapping. Porosity predicted by transformation of AI shows 30 % whereas direct inversion estimates 25 %. Direct inversion of porosity estimation is close in agreement with the actual porosity of Raghavapuram Shale.

5. Conclusions

The direct estimation of porosity from seismic inversion has been implemented using porosity wavelet. The AI and porosity wavelet has the exactly opposite polarity due to negative trend between AI and porosity. This work demonstrated an uncommon porosity prediction methodology from post-stack seismic data. The high impedance zones observed in the seismic section of K-G basin having source rock potential show relatively less porosity compared to the porosity of low impedance zones. Top of Cretaceous is marked by high impedance and low porosity. Sediments of Palaeocene age is observed with low impedance and high porosity. The shales/unconsolidated sediments measure a high porosity with low impedance and the more porous sand are in an intermediate range. This porosity prediction is further to be validated with large numbers of wells or core porosity data in future.

Acknowledgement

Authors are thankful to the Managing Director, GSPCL for their kind approval and sharing of seismic and well log data for academic purposes. The Ministry of Earth Science is acknowledged for providing financial support through the R&D project MoES/P.O./(Seismo)/1(138) 2011 dated 09.11.12.

References

Bateman, R.M., 1985. Openhole Log Analysis and Formation Evaluation, Pretice Hall PTR, New Jersey. 1985. 647 p.

Buiting, J.J. M., Bacon M. Seismic inversion as a vehicle for integration of geophysical, geological and petrophysical information for reservoir characterization: Some North Sea examples. *Petroleum Geology of Northwest Europe: Proceedings of the 5th Conference*. Geological Society, London. 1999. V. 5. Pp. 1271-1280.

Eichkitz C.G., Schreilechner M.G., Amtmann J. and Schmid C. Shallow Seismic Reflection Study of the Gschliefgraben Landslide Deposition Area – Interpretation and Three Dimensional Modeling. *Austrian Journal of Earth Sciences*. 2009. V. 102. Pp. 52-60.

Hampson D., Schuelke J. and Quirein J. Use of multi-attribute transforms to predict log properties from seismic data. *Geophysics*. 2001. V. 66. Pp. 220-236.

Husse M., Feary D.A. Seismic inversion for acoustic impedance and porosity of Cenozoic cool-water carbonates on the upper continental slope of the Great Australian Bight. *Marine Geology*. 2005. V. 215. Pp. 123-134.

Jipa, C.D. Coarsening Upward Sedimentation in the Middle Pontian Dacian Basin, Prograding Shoreline or delta front? *Geo-Eco-Marina*. 2012. V. 18. Pp. 45-64.

Kumar, R., Das, B., Chatterjee, R. and Sain, K.A. Methodology of Porosity Estimation from Inversion of Post-Stack Seismic Data. *Journal of Natural Gas Science and Engineering*. 2016. V. 28. Pp. 356-364.

Leiphart, D.J., Hart, B. S. Comparison of linear regression and a probabilistic neural network to predict porosity from 3D seismic attributes in Lower Brushy Canyon channeled sandstones, southeast New Mexico. *Geophysics*. 2001. V. 66. Pp. 1349-1358.

Leite, E. P., Vidal, A. C., Bueno, J. F. and Duarte, R. D. C. 3D Acoustic Impedance and Porosity Mapping from Seismic Inversion and Neural Networks. *SEG Annual Meeting*. Denver. 2010. Pp. 2226-2230.

Løseth, H., Wensaas, L., Gading, M., Duffaut, K., and Springer, M. Can hydrocarbon source rocks be identified on seismic data? *Geology.* 2011. V. 39. Pp. 1167-1170.

Manmohan, M., Rao, M. R. R., Kamraju, A. V. V. S., and Yalamarty, Y. Origin and Occurrence of Lower Cretaceous High Gamma-High Resistivity (Raghavapuram) Shale – A key stratigraphic sequence for hydrocarbon exploration in Krishna-Godavari Basin. *A.P. Journal of Geological society of India*. 2003. V. 62. Pp. 271-289.

Maver, K. G., Rasmussen, K. B. Seismic inversion for reservoir delineation and description. *Society of Petroleum Engineers. Technical Conference and Exhibition*. Bahrain. 1995. Paper id: SPE 29798.

Padhy, P. K., Das, S. K., and Kumar, A. Krishna-Godavari Continental Rift Basin: Shale Gas and Oil Play Systems. *10th Biennial International Conference & Exposition*. SPG, Kochi. 2013. Paper id: P327.

Pramanik, A. G., Singh V., Vig R., Srivastava A. K., and Tiwary D. N. Estimation of effective porosity using geostatistics and multiattribute transforms: A case study. *Geophysics*. 2004. V. 69. Pp. 352-372.

Prasad, M., Pal-Bathija, A., Johnston, M., Rydzy, M., and Batzle, M. Rock physics of the unconventional. *The Leading Edge*. 2002. V. 28. Pp. 34-38.

Rao, G. N. Sedimenation, stratigraphy, and petroleum potential of Krishna-Godavari basin, East Coast of India. *AAPG Bulletin*. 2001. V. 85. Pp. 1623-1643.

Rasmussen, K. B., Maver, K. G. Direct inversion for porosity of post stack seismic data. *European 3-D Reservoir Modeling Conference*. Stavanger. 1996. Paper id: SPE 35509.

Rider, M. H. The geological interpretation of well logs, 2nd edition. Rider-French Consulting Ltd. 2002. 280 p.

Russell, B., Hampson, D. Comparison of poststack inversion methods. *61St Annual International Meeting, SEG, Expanded Abstracts.* 1991. V. 10. Pp. 876-878.

Shrivastava, C., Ganguly, S. and Khan, Z. Reconstructing Sedimentary Depositional Environment with Borehole Imaging and Core. *International Petroleum Technology Conference: A Case Study from Eastern Offshore India*. Kuala Lumpur, Malaysia. 2008.

Singha, D. K., Chatterjee, R. Detection of Overpressure zones and a Statistical Model for Pore Pressure Estimation from Well Logs in the Krishna-Godavari Basin, India. *Geochemistry, Geophysics, Geosystems.* 2014. V. 15. Pp. 1009-1020.

Singha, D. K., Chatterjee, R., Sen, M. K. and Sain, K. Pore pressure prediction in gas-hydrate bearing sediments of Krishna-Godavari Basin in India. *Marine Geology*. 2014. V. 357. Pp. 1-11.

Walls, J.D., Taner M.T., Taylor G., Smith M., Carr M., Derzhi N., Drummond J., McGuire D., Morris S., Bregar J., and Lakings J. Seismic reservoir characterization of a U.S. Midcontinent fluvial system using rock physics, poststack seismic attributes, and neural networks. *The Leading Edge*. 2002. V. 21. Pp. 428-436.

Wyllie, M. R. J., Gregory, A. R. and Gardner, G. H. F. Elastic wave velocities in heterogeneous and porous media. *Geophysics*. 1956. V. 21. Pp. 40-70.

Information about authors

Baisakhi Das – Junior Research Fellow, Indian Institute of Technology (Indian School of Mines), Dhanbad 826004, India

E-mail: baisakhi.das@gmail.com

Rima Chatterjee – Professor, Department of Applied Geophysics, Indian Institute of Technology (Indian School of Mines), Dhanbad 826004, India

E-mail: rima_c_99@yahoo.com

Manuscript received October 19, 2016